

Molecular Dynamics Study on the Liquid-vapor Interfacial Profiles

Z. J. Wang, M. Chen*, Z. Y. Guo, C. Yang

Department of Engineering Mechanics, Tsinghua University, Beijing 100084, P. R. China

ABSTRACT

Molecular dynamics simulations are carried out to study the thermodynamic properties in the liquid-vapor coexistent systems with liquid-vapor interfaces. The interactions between the particles are modeled with a truncated Lennard-Jones pair potential. The density profile, the temperature profile and the pressure tensor are obtained at two different bulk temperatures. There exist a sharp peak and a little valley at the thin region outside the liquid-vapor interface in the local kinetic energy distribution across the interface. When the system temperature increases, the peak falls down, while the valley rises. The non-equilibrium molecular kinetic energy distribution located at the thin region outside the liquid-vapor interface confirms that though a liquid-vapor interface is in thermostatic equilibrium, it may not be in thermokinetic equilibrium. This kind of molecular kinetic energy distribution may embody the behavior of energy transport between the liquid and the vapor phases.

Keywords: liquid-vapor interface; thermodynamic properties; molecular dynamics.

1. INTRODUCTION

Interface behaviors of liquid-vapor interface are fundamental and significant in a variety of fields of science and engineering. Lots of theoretical and experimental investigations have been carried out on it [1*-8]. However, for the reason of the complexity of interface behaviors, there are special difficulties on some topics of interface research, such as microscopic structure of interface and interfacial profiles in molecular level. With the development of computer ability, it becomes possible to approach the problem and perform “computer experiments” from a molecular level, namely, Molecular Dynamics (MD) and Monte Carlo (MC) simulations. These two computer simulation methods can provide us the fundamental information of the interface, hence, make it possible to carry out in-depth study of interface characteristics.

Over the years, considerable studies have been implemented on the properties of liquid-vapor interface with emphasis on the density and pressure profiles and surface tension with MD and MC [9-17]. Rao et al. [9] investigated the surface structure of a liquid film at two low temperatures. In their report, the density profile and its rms fluctuation is the interest. The simulation showed that the density profiles normal to the film surface were monotonic curves. Besides, the non-constant local temperatures were observed, as shown in Fig.1. It was explained by them that the non-uniformity of the local temperature profiles was due to the fluctuations in the simulation.

* Corresponding author

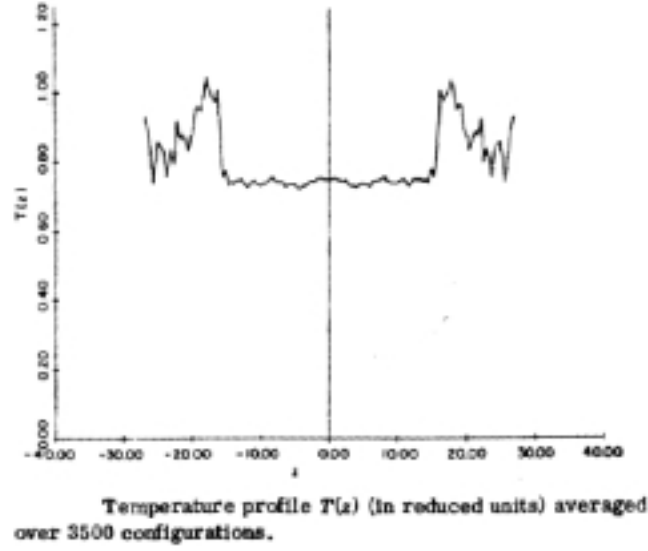


Fig.1. The temperature profile obtained by Rao et al..

Walton et al. [10] calculated the pressure tensor at the planar surface of a liquid. The pressure tensor is a diagonal tensor that is a function only of the height z , and which has the form:

$$P(z) = [\vec{e}_x \vec{e}_x + \vec{e}_y \vec{e}_y] p_T(z) + [\vec{e}_z \vec{e}_z] p_N(z), \quad (1)$$

where \vec{e}_x , \vec{e}_y and \vec{e}_z are orthogonal unit vectors, $p_N(z)$ and $p_T(z)$ are the normal and transverse components. Walton's results showed that in planar interface, the normal component $p_N(z)$ was constant and equals to the saturation pressure, while the difference of the two components of the pressure tensor, $p_N(z) - p_T(z)$, had a variation.

Nijmeijer et al. [11] investigated the surface tension of liquid-vapor interface with Lennard-Jones potential by MD simulation. Their values tended to be smaller than those from previous simulations, which showed that the usually truncated tail of the potential could increase the surface tension if taken into account.

Shukal and Robert [12] studied the structure of the interface between two-dimensional fluid phases with MD simulation. The density profile and the thickness of the vapor-liquid interface were obtained over a range of temperatures. In their report, the exponent describing the divergence of the interfacial thickness at the critical point was determined and compared with theoretical predictions.

Holcomb et al. [13] studied the surface tension and density profiles of the liquid-vapor interface using molecular dynamics simulation for a variety of system sizes, film thicknesses, interfacial areas, interatomic potential cut-offs, and bulk temperatures. They suggested some criteria for obtaining more accurate results for the pure components.

In all above mentioned works [9-16], the temperature in the interface was assumed to be constant and equal to the saturation temperature. However, in the simulation of the interface of a micro liquid droplet, Yang et al. [17] detected that there exists a non-uniform temperature profile.

In this presentation, by using MD method, the thermodynamic properties of the planar liquid-vapor interface, such as density, pressure tensor and temperature profiles,

are studied. Moreover, related interface structure and interphase transport are considered to interpret the non-uniform temperature distribution.

2. SIMULATION

Argon atoms with intermolecular interaction expressed by the 12-6 Lennard-Jones potential are used to model a planar interface in the state of equilibrium. The Lennard-Jones potential has the form:

$$U(r) = 4\varepsilon \left[\left(\frac{\sigma}{r} \right)^{12} - \left(\frac{\sigma}{r} \right)^6 \right], \quad (2)$$

where r is the molecular pair separation, and parameters of the potential are $\sigma = 3.405 \times 10^{-10} \text{ m}$, $\varepsilon = 1.67 \times 10^{-21} \text{ J}$.

The initial positions of argon atoms are arranged in the middle of the quadrate box where the initial distance between argon atoms is the average distance of saturated liquid atoms. In the simulation, the total number of molecules (N), the volume (V) and the bulk temperature (T) are fixed. The cut-off distance is 3.0σ , and the time step is $0.5 \times 10^{-15} \text{ s}$. Periodic boundary conditions are used in all three directions. In order to obtain stable profiles, The length in z direction of the simulation systems is designed large enough to have adequate vapor phase space. The size of the liquid film is designed to be greater than 12σ . This lower limit on the thickness of the film is designed to prevent particles on one side of the film from being within the intermolecular potential range of any particle on the opposite side of the film and to ensure that a truly liquid-vapor interface is produced. When equilibrium is achieved, the system with a planar interface inside is obtained.

300,000 steps are used to obtain the simulated system of planar interface, the final 100,000 steps are used to statistic the density, the two components of the pressure tensor and the local temperature profiles. When equilibrium achieved, not only the system's energy and the number of vapor atoms are settled to constant levels, but also the running average for the pressure tensor and density profile must not be changing significantly. The simulation running time necessary to reach equilibrium appears to be considerably long, furthermore, statistical time steps necessary to obtain stable profiles must be adequate. Therefore, in order to obtain reliable results, much long time of simulation is needed.

The following expressions are used to calculated the temperature and the two components of the pressure tensor respectively:

$$T(z) = \frac{1}{3kn(z)} \sum_{i=1}^{n(z)} (mv_i^2), \quad (3)$$

$$p_N(z) = n(z)kT(z) - \frac{1}{2A} \left(\sum_{i<j} \frac{z_{ij}^2}{r_{ij}} U'(r_{ij}) \frac{1}{|z_{ij}|} \theta\left(\frac{z-z_i}{z_{ij}}\right) \theta\left(\frac{z_j-z}{z_{ij}}\right) \right), \quad (4)$$

$$p_T(z) = n(z)kT(z) - \frac{1}{4A} \left(\sum_{i<j} \frac{x_{ij}^2 + y_{ij}^2}{r_{ij}} U'(r_{ij}) \frac{1}{|z_{ij}|} \theta\left(\frac{z-z_i}{z_{ij}}\right) \theta\left(\frac{z_j-z}{z_{ij}}\right) \right), \quad (5)$$

$$\theta(x) = \begin{cases} 1 & (x \geq 0) \\ 0 & (x < 0) \end{cases}. \quad (6)$$

The $\sum_{i=1}^{n(z)}$ notation indicates a summation over all the particles in height z , and the $\sum_{i<j}$ notation indicates a summation over all distinct pairs i and j without counting any pair twice (i.e. as ij and ji). $n(z)$ is the number density in height z , and k is the Boltzmann's constant. m represents the mass of a molecule, and v_i represents the velocity of i molecule. r_{ij} is the molecular separation of the pair i and j , which is equal to $\sqrt{x_{ij}^2 + y_{ij}^2 + z_{ij}^2}$.

In the simulations, reduced parameters are used: the reduced components of the pressure tensor are $p_N^* = \frac{p_N \sigma^3}{24\epsilon}$, $p_T^* = \frac{p_T \sigma^3}{24\epsilon}$, the reduced height $z^* = \frac{z}{\sigma}$, the reduced number density $n^* = n \sigma^3$.

3. RESULTS AND DISCUSSION

The local density profiles at 130K and 83.78K are given in Fig.2. As shown in the figure, according to the density variation in space, the simulated systems can be divided into three regions, namely the liquid region, the transition/interface region and the vapor region. The higher the system temperature, the thicker is the transition region and the smaller is the difference of the density between the liquid and the vapor.

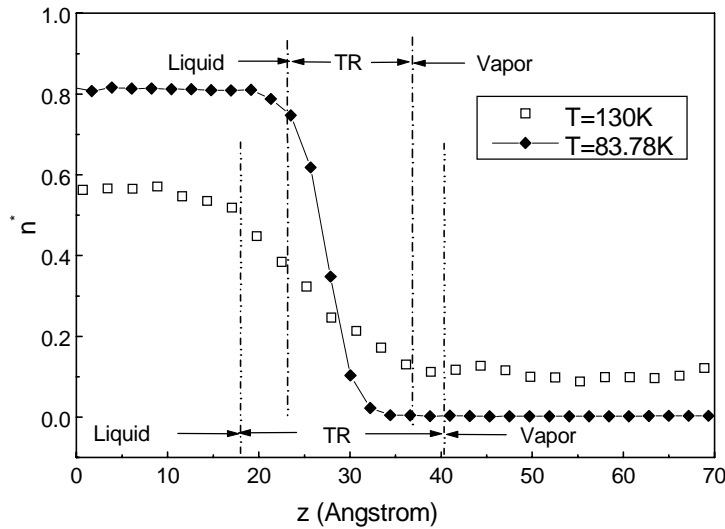


Fig.2. The profiles of densities at two different saturation temperatures.

The density profile, the reduced normal and transverse component profiles of the pressure tensor and the local temperature profile at 83.78K are given in Fig.3. The normal component of the pressure tensor is a constant value equal to the saturation pressure of the system. However, the transverse component $p_T(z)$ is not a constant value, thereby a nonzero $p_N(z) - p_T(z)$ distribution in the interface region which causing the surface tension exists. The planar interface at 130K is also simulated, and the results show that the peak value of $p_N^*(z) - p_T^*(z)$ decreases when the bulk temperature

increases, meanwhile, the surface tension falls down, which is consistent with the results in the previous simulations.

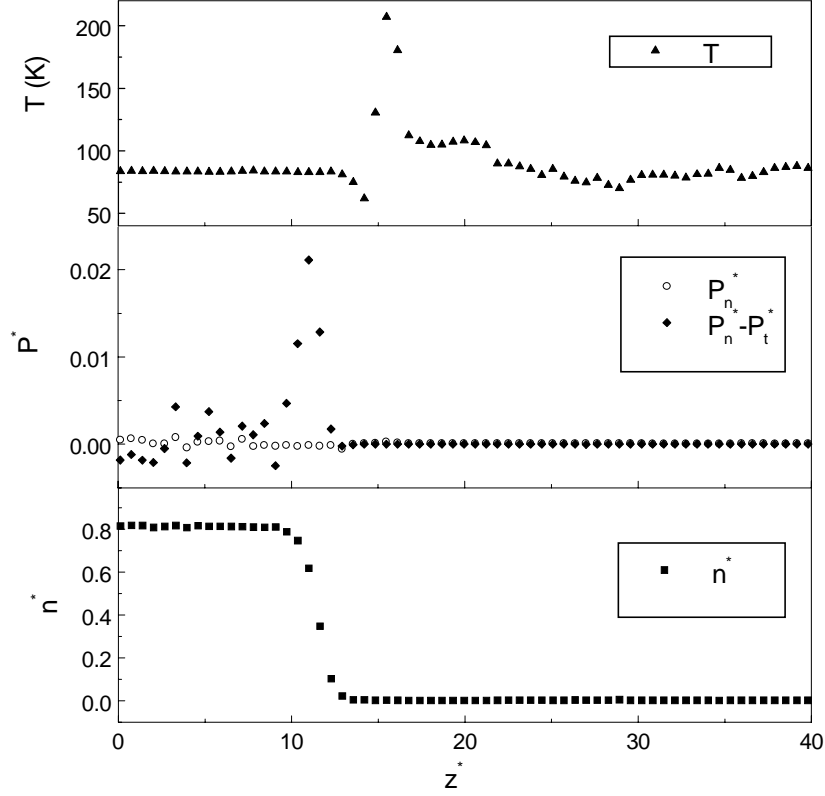


Fig.3. The interfacial profiles of density, pressure tensor components and local temperature (83.78K).

As shown in Fig.3, the local temperature is not constant and equal to the saturation temperature as supposed in most previous literature. There exists a peak located about 2σ outside the transition region in the local temperature profile of liquid-vapor interface. It could also be seen from the figure that in the temperature profile there seems to be a little valley before the peak. The magnitude of the observed valley is nearly in the same order of the simulation fluctuation, so the valley is prone to be submerged in the fluctuation, especially at high system temperature. Moreover, to the peaks in the local temperature profile, it is shown that the lower the temperature, the higher is the peak. When the system temperature is 130K, the magnitude of the peak is nearly at the same order of the statistical fluctuation.

From the macroscopic arguments, it is usually considered that the temperature is a constant value equal to the saturation temperature for a system at thermodynamic equilibrium [9-16,18]. However, as being pointed out in some literature [19], the condition close to the surface may not be in static thermal equilibrium. It is confirmed by our simulations, in which the non-uniform distribution of the temperature profile through the interface is observed. It means that for the reason of evaporation and condensation, though a liquid-vapor interface is in thermostatic equilibrium, it may not

be at thermokinetic equilibrium in a limited region near the liquid-vapor interface and may show non-uniform thermodynamic parameters through the interface in a molecular level investigation.

The liquid-vapor interface is a wavy surface varying with time, as show in Fig.4, which may be expressed as function $z = f(x, y, t)$. The density profile and the interface position at fixed (x_0, y_0) , $z = f(x_0, y_0, t)$, is given in Fig.5. The figure indicates that width of the transition region is equal to the magnitude of the fluctuation of the liquid-vapor interface along with time, i.e. the transition region is the undulant region of the interface varying with time. The gradual change of the thermodynamic quantity (e.g. pressure, density and so forth) is the statistical results.

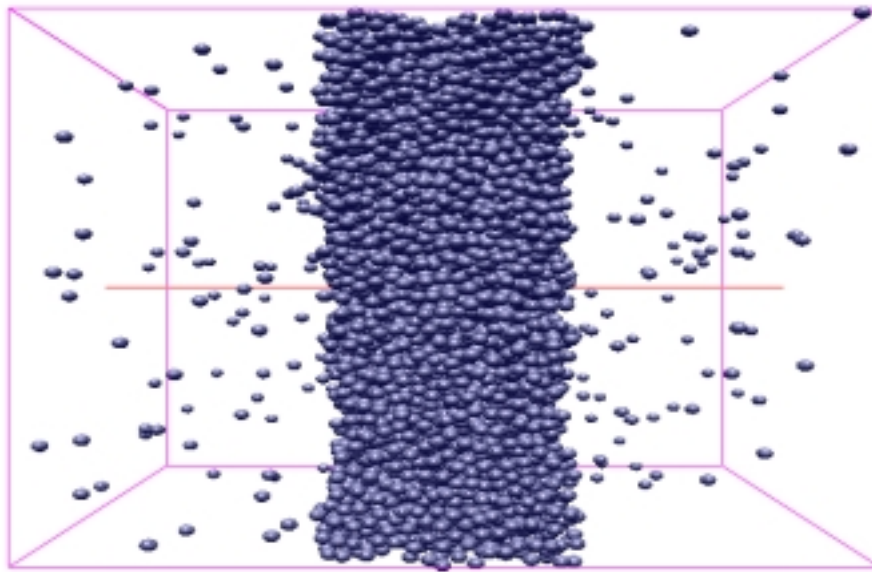


Fig.4. The wavy liquid-vapor interface (83.78K).

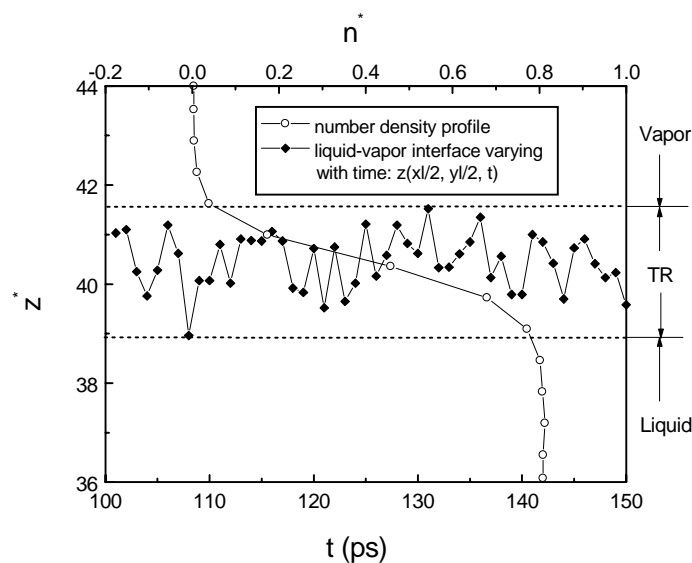


Fig.5. The profile of density and the interface position fluctuating with time (83.78K).

When colliding with the wavy liquid-vapor interface, a particle is coming into the process of evaporation, condensation or reflection. In any of the three processes, there must be a remarkable change of kinetic energy for the particle, as presented in literature [20,21]. As shown in Fig.6, for the gaseous molecules close to the liquid-vapor interface, there are ceaseless energy transfers between them and the liquid-vapor interface. Furthermore, for the reason of the low number density outside the liquid-vapor interface, the mean free path of the gaseous molecule is reasonably long. Energy transport in the gaseous phase needs some space distance, which causes the non-equilibrium molecular kinetic energy distribution in a limited gaseous space outside the liquid-vapor interface. This kind of molecular kinetic energy distribution exhibits the energy transport between the liquid and the vapor phases. The region in which there exists a non-equilibrium molecular kinetic energy distribution is very thin, only several molecular diameters wide. In macroscopic thermodynamics, the non-equilibrium molecular kinetic energy distribution in such a thin region may not be considered. However, it may have important effects on recognizing microscopic liquid-vapor phase change processes and estimating phase change rate.

When the temperature rises, the difference of the density between the liquid and the vapor decreases. The mean free path of the gaseous molecule decreases, on the other hand, the kinetic energy variation begotten by the moving from one phase to the other falls down. Therefore, the non-uniformity of average kinetic energy in the thin region outside the liquid-vapor interface gets invisible.

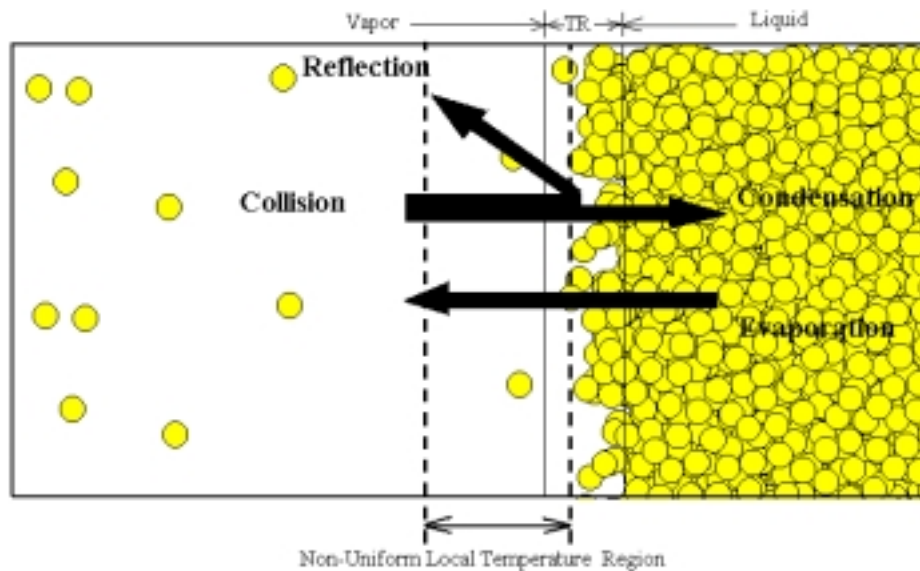


Fig.6. Liquid-vapor interface and related interphase transport

4. CONCLUSIONS

The planar liquid-vapor interface of argon modeled by a Lennard-Jones pair potential has been simulated at two bulk temperatures by the molecular dynamics method. The interface profiles of the density, the normal and transverse components of the pressure tensor, and the local temperature are obtained at equilibrium.

The density and the pressure tensor profiles exhibit the same laws as the previous research. However, there exists a sharp peak and a little valley in the local temperature profile, i.e. there exists a non-equilibrium molecular kinetic energy distribution through

the interface.

This reveals that a non-equilibrium molecular kinetic energy distribution is begotten in the gaseous phase space close to the liquid-vapor interface. The non-equilibrium kinetic energy region is only several molecular diameters wide. Meanwhile, the higher the saturation temperature of the system, the more invisible is the non-equilibrium of molecular kinetic energy in the thin region outside the liquid-vapor interface. The non-equilibrium molecular kinetic energy distribution located in the thin region outside the liquid-vapor interface confirms that though a liquid-vapor interface is in thermostatic equilibrium, it may not be in thermokinetic equilibrium. This kind of average kinetic energy distribution embodies the energy transport between the liquid and the vapor phases.

ACKNOWLEDGEMENTS

The supports from the National Natural Science Foundation of China under Grand Number 59876016, the High Technology Research and Development Program (863 program) of China Government, the Fundamental Research Foundation, the Doctoral Education Foundation and the Tong-Fang Computational Foundation of Tsinghua University are gratefully acknowledged.

REFERENCES

1. K. Lunkenheimer, R Hirte, *J. Phys. Chem.*, 96 (1992) 8683-8686.
2. H. T. Davis, L. E. Scriven, *Adv. Chem. Phys.*, 49 (1982) 357-454.
3. P. M. W. Cornelisse, C. J. Peters, J. de Swaan Arons, *Fluid Phase Equilibria*, 82 (1993) 119-129.
4. S. Toxvaerd, *J. Chem. Phys.*, 55 (1971) 3116-3120.
5. P. I. Teixeira, M. M. Telo da Gama, *J. Phys. Condens. Matter*, 3 (1991) 111-125.
6. J. Winkelmann, U. Brodrecht, I. Kreft, *Ber. Bunsen. Phys. Chem.*, 98 (1994) 912-919.
7. J. J. Jasper, *J. Phys. Chem. Ref. Data*, 1 (1972) 841-1009.
8. K. B. Eisenthal, *Annu. Rev. Phys. Chem.*, 43 (1992) 627-661.
9. M. Rao, and D. Levesque, *J. Chem. Phys.*, 65 (1976) 3233-3236.
10. J. P. R. B. Walton, D. J. Tildesley, and J. S. Rowlinson, *Mol. Phys.*, 48 (1982) 1357-1368.
11. M. J. P. Nijmeijer, A. F. Bakker, C. Bruin, and J. H. Sikkenk, *J. Chem. Phys.*, 89 (1988) 3789-3792.
12. K. P. Shukal, and M. Robert, *Fluid Phase Equilibria*, 79 (1992) 139-149.
13. C. D. Holcomb, P. Clancy, and J. A. Zollweg, *Mol. Phys.*, 78 (1993) 437-459.
14. K. S. Liu, *J. Chem. Phys.*, 60 (1974) 4226-4230.
15. F. F. Abraham, S. E. Schreiber, J. A. Barker, *J. Chem. Phys.*, 62 (1975) 1958-1960.
16. P. Attard, and G. A. Moule, *Mol. Phys.*, 78 (1993) 943-959.
17. C. Yang, M. Chen, Z. Y. Guo, *Chin. Phys. Lett.*, 16 (1999) 803-804.
18. H. K. Cammenga, *Current Topics in Materials Science 5*, North-Holland, Amsterdam, 1980, pp. 339-341.
19. J. G. Collier, J. R. Thome, *Convective Boiling and Condensation*, Clarendon, Oxford, 3rd ed., 1994, pp 433-434.
20. M. Matsumoto, Y. Kataoka, *Phys. Rev. Lett.*, 69 (1992) 3782-3784.
21. T. Tsuruta, H. Tanaka, T. Masuoka, *International Journal of Heat and Mass Transfer*, 42 (1999) 4107-4116.